

Supporting Information

Intervalley Scattering of Interlayer Excitons in a MoS₂/MoSe₂/MoS₂ Heterostructure in High Magnetic Field

Alessandro Surrente,[†] Łukasz Kłopotowski,[‡] Nan Zhang,[†] Michal Baranowski,^{†,¶}
Anatolie A. Mitioglu,[§] Mariana V. Ballottin,[§] Peter C. M. Christianen,[§] Dumitru
Dumcenco,^{||} Yen-Cheng Kung,^{||} Duncan K. Maude,[†] Andras Kis,^{||} and Paulina
Plochocka^{*,†}

[†]*Laboratoire National des Champs Magnétiques Intenses, UPR 3228,
CNRS-UGA-UPS-INSA, 38042 Grenoble and 31400 Toulouse, France*

[‡]*Institute of Physics, Polish Academy of Sciences, Al. Lotników 32/46, 02-668 Warsaw,
Poland*

[¶]*Department of Experimental Physics, Faculty of Fundamental Problems of Technology,
Wrocław University of Science and Technology, 50-370 Wrocław, Poland*

[§]*High Field Magnet Laboratory (HFML – EMFL), Radboud University, 6525 ED Nijmegen,
The Netherlands*

^{||}*Electrical Engineering Institute and Institute of Materials Science and Engineering, École
Polytechnique Fédérale de Lausanne, CH-1015 Lausanne, Switzerland*

E-mail: paulina.plochocka@lncmi.cnrs.fr

Photoluminescence and reflectivity contrast spectra in the absence of magnetic field

Samples grown by chemical vapour deposition (CVD) are generally characterized by a broad emission resulting from the recombination of excitonic species bound to impurities, primarily related to chalcogen vacancies.¹ At low temperatures, the free exciton peak is barely visible in photoluminescence (PL) as a shoulder on the high energy side of a broad emission. These defects can be healed by hydrohalic acid treatment¹ or, as we demonstrated, by sandwiching CVD-grown MoSe₂ between two CVD-grown MoS₂ monolayers.² Our defect healed samples exhibit dramatically improved quality, as demonstrated by the low temperature micro-photoluminescence (μ PL) spectrum shown in Fig. S1. The spectrum consists of sharp, well-resolved peaks at 1.67 eV and 1.64 eV, identified with the free and charged exciton of MoSe₂, respectively. The defect healing scenario is confirmed by the strongly suppressed luminescence of the excitons bound to defects. The peak at 1.95 eV is assigned to the recombination of the A exciton of MoS₂. The prominent low energy peak in Fig. S1 is attributed to the interlayer exciton based on extensive power dependent PL measurements, PL excitation spectroscopy, and time-resolved PL measurements.³ The high quality of our heterostructure is confirmed by the reflectivity contrast spectrum, where peaks attributed to A and B excitons of both MoS₂ and MoSe₂ are distinctly resolved.²

Valley Zeeman splitting for intralayer and interlayer excitons

The lifting of the degeneracy induced by the magnetic field is enabled by the unequal magnetic moments of the conduction μ^c and valence bands μ^v involved in the transition. In the framework of magneto-optical spectroscopy of intralayer excitons, three possible contributions have been identified. The contributions related to the spin magnetic moment $\mu_s^{c,v}$

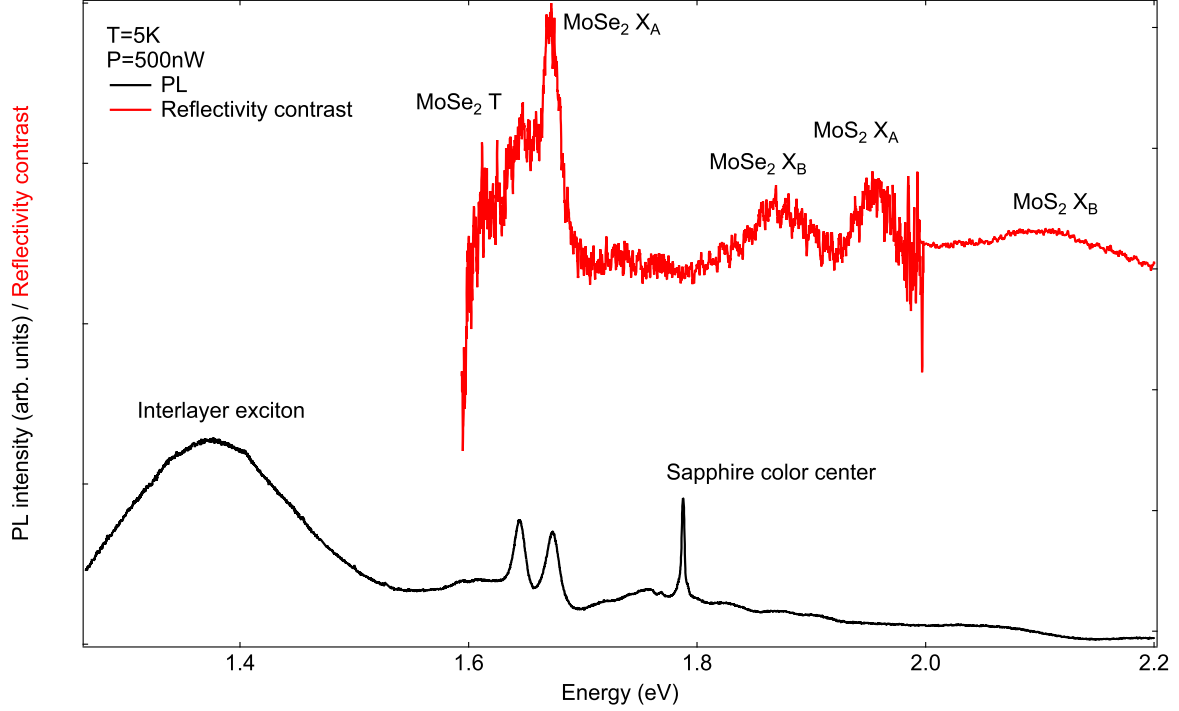


Figure S1: μ PL spectrum measured at low excitation power and low temperature and reflectivity contrast spectrum of a $\text{MoS}_2/\text{MoSe}_2/\text{MoS}_2$ trilayer.

cancel out because optical transitions are spin-conserving, leading to $\mu_s^c = \mu_s^v$. Conversely, the atomic orbital contribution μ_l is expected to be non-zero, owing to the different orbitals which form the band edge states of the conduction and the valence band,⁴ with a total contribution adding up to $\mu_l = -4\mu_B$. The third contribution is associated with the Berry curvature and is referred to as valley magnetic moment,⁵ with values $\pm\mu_k^c = \pm(m_0/m_e)\mu_B$ for the conduction band and $\pm\mu_k^v = \pm(m_0/m_h)\mu_B$ for the valence band, in the K^+ and K^- valleys, respectively. Here, m_0 represents the free electron mass, while m_e and m_h denote the effective mass of the electrons and holes, respectively. In first approximation, a simple tight binding model yields $m_e = m_h$, hence $\mu_k^c = \mu_k^v$ for transitions occurring between bands belonging to the same valley. The valley magnetic moment thus provides a negligible contribution, which is consistent with the experimentally observed splitting of the free exciton transition of $\Delta E = -4\mu_B B$ in the vast majority of the magneto-optical experiments performed on monolayer TMDs.⁶⁻⁹ In heterostructures, an appropriate choice of the stacking angle or the effects of moiré pattern

can enable optically bright transitions between bands having different valley indices. The very large effective g -factor observed in a MoSe₂/WSe₂ heterostructure has been explained by the $\sim 60^\circ$ stacking angle between the monolayers, which made possible optically bright transitions between K⁺ valley of MoSe₂ and K⁻ valley of WSe₂ (and vice versa).¹⁰ In this configuration, the valley orbital contribution will no longer cancel out, but it will add up leading to an expected splitting $\Delta E = -[4 + 2(m_0/m_e + m_0/m_h)]\mu_B B$. In the case of MoS₂/MoSe₂ heterostructures, the optically active transition involve the highest energy conduction band of MoS₂ of one valley and the valence band of MoSe₂ of the opposite valley [see Fig. 1(b)]. Theoretical calculations suggest values of the effective mass of electrons in MoS₂ ranging from $m_e \sim 0.46m_0 - 0.6m_0$ and of holes in MoSe₂ from $m_h \sim 0.55m_0 - 0.6m_0$,^{11,12} which gives an expected $g_{\text{eff}} \sim 11 - 11.6$, in good agreement with the experimentally determined value.

Determination of PL energy

Even though the zero field PL spectrum shown in Fig. 1(b) has a slightly uneven line shape, its peak energy and intensity can be reliably extracted by fitting it with a single Gaussian curve. We show an example of a single Gaussian fit in Fig. S2(a), where we note that the fitting Gaussian follows very well the PL line shape even at its tails. This demonstrates that our spectra are not asymmetric and the spectral information can be reliably extracted by fitting them with a single curve. Recent reports have demonstrated two well-resolved peaks attributed to the interlayer exciton recombination.^{13,14} To check whether the structure we see in our spectra could be related to the presence of two peaks, we try to fit the zero field spectrum with two Gaussians. The result, shown in Fig. S2(b), demonstrates that the central energies of the two Gaussians are very close to each other (1.3799 eV and 1.3833 eV) and very close to the energy we extracted with a single curve fit (1.3824 eV), hence we conclude that our spectra can be fitted well with a single Gaussian and that the effective g -factor

extracted with this approach in Fig. 1(d) is correct.

We have also extracted the magnetic field induced energy splitting with the center of mass method, which gives the energy of a PL peak by evaluating its “weighted spectral average”¹⁵

$$\frac{\sum EI(E)}{\sum I(E)},$$

where E is the energy and $I(E)$ denotes the PL intensity at the energy E . The results of this analysis are summarized in Fig. S2(c). We note that for large magnetic fields ($B > 20$ T), the values of the splitting are more scattered, which reflects a larger uncertainty in the determination of the PL peak because of the very weak signal of the σ^- polarization. Nevertheless, the g_{eff} we obtained using this approach is identical within experimental error to the value we extracted in Fig. 1(d).

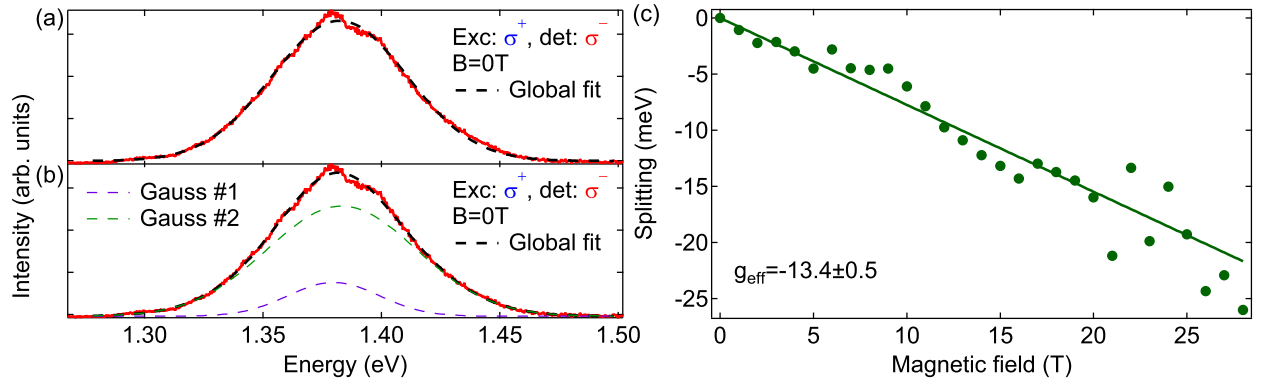


Figure S2: Zero magnetic field spectra fitted with (a) one and (b) two Gaussians. (c) Magnetic field induced energy splitting evaluated via the “center of mass” method.

Four level rate equations model and additional fits

To reproduce the magnetic field dependence of the circular polarization degree P_c of the interlayer exciton photoluminescence (PL), we employ a simple, four level rate equations model. The same model was used by Aivazian *et al.* and Neumann *et al.* to evaluate the magnetic field dependence of P_c of excitonic PL from a WSe₂ monolayer.^{16,17} The schematic of the model is depicted in Fig. 4(d) of the main text and we redraw it in Fig. S3, labeling

the states with numbers for the sake of notation clarity. It shows the case of σ^+ -polarized excitation in resonance with monolayer MoSe₂ or MoS₂ A-exciton, state $|3\rangle$. According to the selection rules,⁵ σ^+ -polarized excitation creates the excitons solely in the K⁺ valley of the monolayer. After photoexcitation, occurring with a rate γ_{03} , a charge transfer between the layers takes place, resulting in a formation of one of the interlayer exciton states, labeled as $|1\rangle$ and $|2\rangle$ (corresponding to the $|\uparrow\rangle$ and $|\downarrow\rangle$ states in the main text). Simultaneously, a partial valley depolarization occurs either between the monolayer states¹⁸ or during the charge transfer.¹⁹ We describe the valley specific charge transfer rates with γ_{31} and γ_{32} . The interlayer exciton states are split in an external magnetic field B perpendicular to the heterostructure surface and the splitting $\Delta E = g_{\text{eff}}\mu_B B$ scales with $g_{\text{eff}} = -13.1$, as determined experimentally and described in the main text. Intervalley scattering rate to the low energy state $|1\rangle$ is γ_{21} , while the scattering to the high energy state $|2\rangle$ is γ_{12} . At zero field, the time reversal symmetry requires that $\gamma_{21} = \gamma_{12}$. These processes compete with the recombination of the interlayer exciton, which occurs with a rate γ , assumed the same for the two valley states. The full set of rate equations describing the populations of the $|3\rangle$, $|2\rangle$, $|1\rangle$ states and the ground state $|0\rangle$ in a steady state reads

$$\begin{aligned}
\dot{n}_3 &= \gamma_{03}n_0 - \gamma_{31}n_3 - \gamma_{32}n_3 = 0 \\
\dot{n}_2 &= \gamma_{32}n_3 - \gamma_{21}n_2 + \gamma_{12}n_1 - \gamma n_2 = 0 \\
\dot{n}_1 &= \gamma_{31}n_3 + \gamma_{21}n_2 - \gamma_{12}n_1 - \gamma n_1 = 0 \\
\dot{n}_0 &= \gamma n_2 + \gamma n_1 - \gamma_{03}n_0 = 0
\end{aligned} \tag{1}$$

where \dot{n}_i denotes the time derivative of the $|i\rangle$ state population. Note that the form of the above equations does not depend on the excitation polarization.

We solve the above set of equations and denote $P_0 = (\gamma_{31} - \gamma_{32})/(\gamma_{31} + \gamma_{32})$ as the degree of polarization transmitted from the excitation light through excitation of the monolayer

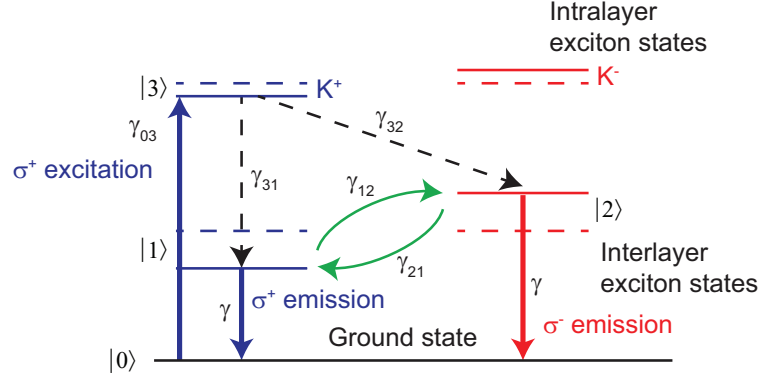


Figure S3: Schematic of the four level rate equations model. Dashed and solid horizontal lines denote the relevant exciton states at $B = 0$ and at $B > 0$, respectively. Circularly polarized excitation with rate γ_{03} (thick upward arrow), creates excitons in one of the valleys in one of the monolayers. Charge transfer and formation of interlayer excitons are partially valley selective, which is accounted for with different rates γ_{32} and γ_{31} (dashed arrows). The intervalley scattering between the interlayer states is described by the rates γ_{12} and γ_{21} (curved arrows). The recombination rate γ of the interlayer exciton (thick downward arrows) is assumed to be the same for both valleys.

exciton, charge transfer, and interlayer exciton formation. The solution for the magnetic field dependence of P_c is given by Eq. (1) of the main text:

$$P_c = P_0 \frac{\gamma}{\gamma + \gamma_{21} + \gamma_{12}} + \frac{\gamma_{21} - \gamma_{12}}{\gamma + \gamma_{21} + \gamma_{12}}. \quad (2)$$

At zero field, the first term reduces to the well known expression for optically created PL polarization related to a spin or valley polarization²⁰

$$P_c = P_0 \frac{\tau_v}{\tau_v + \tau_r}, \quad (3)$$

where $\tau_r = 1/\gamma$ is the recombination time, while $\tau_v = 1/(\gamma_{21} + \gamma_{12})$ is the intervalley scattering time.

Following the approach used successfully to reproduce magnetic field dependence of P_c

in quantum wells,^{21,22} we calculate the valley relaxation rates as:

$$\begin{aligned}\gamma_{21} &= \frac{1}{\tau_{v0}} \frac{\Gamma^2}{\Gamma^2 + \Delta E^2} + \alpha \Delta E^3 \frac{\exp\left(\frac{\Delta E}{k_B T}\right)}{\left|\exp\left(\frac{\Delta E}{k_B T}\right) - 1\right|} \\ \gamma_{12} &= \frac{1}{\tau_{v0}} \frac{\Gamma^2}{\Gamma^2 + \Delta E^2} + \alpha \Delta E^3 \frac{1}{\left|\exp\left(\frac{\Delta E}{k_B T}\right) - 1\right|},\end{aligned}\quad (4)$$

which is equivalent to Eq. (2) of the main text. As discussed therein, the first terms describe the intervalley scattering driven by the electron-hole exchange interaction.

The second terms in Eq. (4) describe a one-phonon spin-lattice relaxation process, which appears only when the valley splitting ΔE is non-zero. The rate γ_{21} describes the scattering from the higher to the lower valley and thus requires an emission of a phonon, while γ_{12} describes the scattering from the lower to the higher valley and requires phonon absorption. Consequently, as seen in Eq. (4), the scattering rates γ_{21} and γ_{12} are proportional to phonon occupation factors $n_k + 1$ and n_k , respectively, and $n_k = \left|\exp\left(\frac{\Delta E}{k_B T}\right) - 1\right|^{-1}$. The spin-lattice relaxation drives the system to thermal equilibrium: the ratio of the phonon contributions to γ_{21} and γ_{12} is equal to the Boltzmann factor $\exp(\Delta E/(k_B T))$.

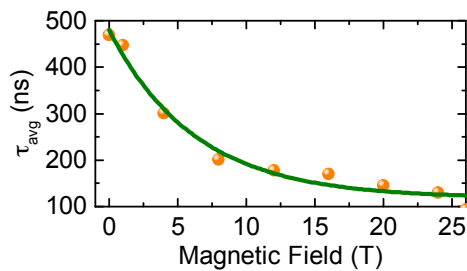


Figure S4: Symbols: average recombination time evaluated from the decay times measured in time-resolved PL (see Fig. 4 of the main text). Line: fitted exponential function $A \exp(-B/B_x) + C$ used for interpolation of the decay time in model fitting.

As described in the main text, the recombination rate γ is evaluated directly from time-resolved PL measurements by calculating the average recombination time τ_{avg} . In Fig. S4, we plot the obtained values of τ_{avg} as a function of the magnetic field. To calculate the magnetic field dependence of P_c in the steady state measurement, we interpolate τ_{avg} with

a fitted exponential function $A \exp(-B/B_x) + C$ – see Fig. S4. The fitting parameters are $A = 362$ ns, $B_x = 6.29$ T, and $C = 118$ ns.

In order to further demonstrate the agreement between our model and the experimental result, we analyze P_c of the PL signal excited in resonance with the MoS₂ A-exciton. In this case, the excitation energy is ~ 260 meV higher than in the case presented in Fig. 2 of the main text. We plot P_c obtained by exciting with a linear polarization in Fig. S5(a) and with σ^\pm polarizations in Fig. S5(b,c), respectively. Qualitatively, the field dependence of P_c observed in Fig. S5 is very similar to that of Fig. 2, except for smaller values of the optically created valley polarization manifested at fields $0 < B < 5$ T for σ^\pm excitations. We fit the experimental data with Eq. (2) and we keep τ_{v0} , α , and Γ obtained from fitting the data in Fig. 2 and use only P_0 as the fitting parameter. For $P_0 = 0.07$, we obtain a very good agreement between the fit and the data.

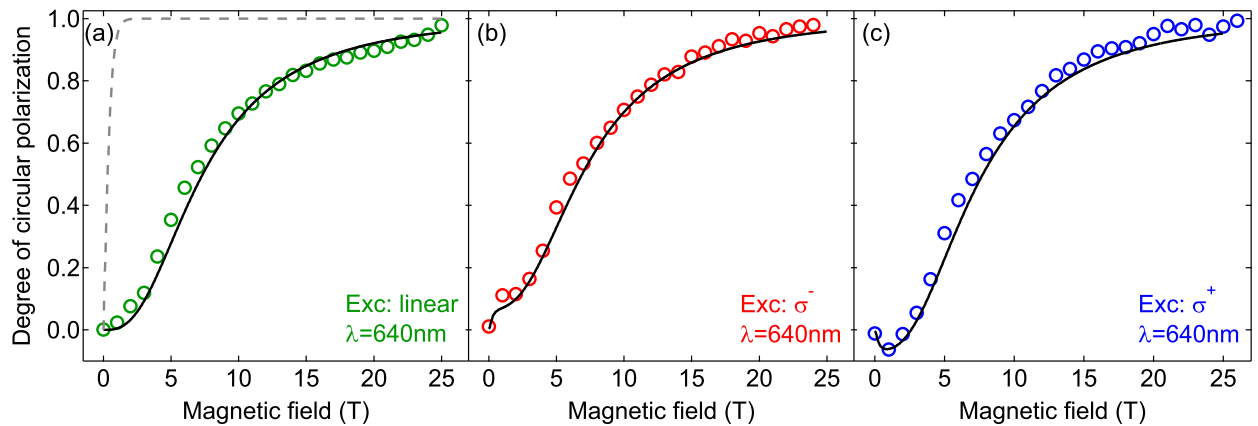


Figure S5: Results of a measurement analogous to the one presented in Fig. 2 of the main text but with the excitation resonant with the MoS₂ A exciton. Symbols denote the evolution of PL circular polarization with magnetic field for (a) linearly polarized excitation, (b) σ^- , and (c) σ^+ polarized excitation. The dashed gray line shows the expected evolution of the circular polarization for an exciton population fully thermalized with the lattice. Lines are results of the fitting with the four level rate equations model.

References

- (1) Han, H.-V.; Lu, A.-Y.; Lu, L.-S.; Huang, J.-K.; Li, H.; Hsu, C.-L.; Lin, Y.-C.; Chiu, M.-H.; Suenaga, K.; Chu, C.-W.; Kuo, H.-C.; Chang, W.-H.; Li, L.-J.; Shi, Y. Photoluminescence enhancement and structure repairing of monolayer MoSe₂ by hydrohalic acid treatment. *ACS Nano* **2016**, *10*, 1454–1461.
- (2) Surrente, A.; Dumcenco, D.; Yang, Z.; Kuc, A.; Jing, Y.; Heine, T.; Kung, Y.-C.; Maude, D. K.; Kis, A.; Plochocka, P. Defect healing and charge transfer mediated valley polarization in MoS₂/MoSe₂/MoS₂ trilayer van der Waals heterostructures. *Nano Letters* **2017**, *17*, 4130–4136.
- (3) Baranowski, M.; Surrente, A.; Klopotoski, L.; Urban, J.; Zhang, N.; Maude, D. K.; Wiwatowski, K.; Mackowski, S.; Kung, Y.-C.; Dumcenco, D.; Kis, A.; Plochocka, P. Probing the Interlayer Exciton Physics in a MoS₂/MoSe₂/MoS₂ van der Waals Heterostructure. *Nano Letters* **2017**, *17*, 6360–6365.
- (4) Liu, G.-B.; Shan, W.-Y.; Yao, Y.; Yao, W.; Xiao, D. Three-band tight-binding model for monolayers of group-VIB transition metal dichalcogenides. *Physical Review B* **2013**, *88*, 085433.
- (5) Xiao, D.; Liu, G.-B.; Feng, W.; Xu, X.; Yao, W. Coupled spin and valley physics in monolayers of MoS₂ and other group-VI dichalcogenides. *Physical Review Letters* **2012**, *108*, 196802.
- (6) Li, Y.; Ludwig, J.; Low, T.; Chernikov, A.; Cui, X.; Arefe, G.; Kim, Y. D.; van der Zande, A. M.; Rigosi, A.; Hill, H. M.; Kim, S. H.; Hone, J.; Li, Z.; Smirnov, D.; Heinz, T. F. Valley Splitting and Polarization by the Zeeman Effect in Monolayer MoSe₂. *Physical Review Letters* **2014**, *113*, 266804.
- (7) Srivastava, A.; Sidler, M.; Allain, A. V.; Lembke, D. S.; Kis, A.; Imamoglu, A. Valley

- Zeeman effect in elementary optical excitations of monolayer WSe_2 . *Nature Physics* **2015**, *11*, 141–147.
- (8) MacNeill, D.; Heikes, C.; Mak, K. F.; Anderson, Z.; Kormányos, A.; Zólyomi, V.; Park, J.; Ralph, D. C. Breaking of valley degeneracy by magnetic field in monolayer MoSe_2 . *Physical Review Letters* **2015**, *114*, 037401.
- (9) Plechinger, G.; Nagler, P.; Arora, A.; Granados del Águila, A.; Ballottin, M. V.; Frank, T.; Steinleitner, P.; Gmitra, M.; Fabian, J.; Christianen, P. C.; Bratschitsch, R.; Schüller, C.; Korn, T. Excitonic valley effects in monolayer WS_2 under high magnetic fields. *Nano Letters* **2016**, *16*, 7899–7904.
- (10) Nagler, P.; Ballottin, M. V.; Mitioglu, A. A.; Mooshammer, F.; Paradiso, N.; Strunk, C.; Huber, R.; Chernikov, A.; Christianen, P. C.; Schüller, C.; Korn, T. Giant magnetic splitting inducing near-unity valley polarization in van der Waals heterostructures. *Nature Communications* **2017**, *8*, 1551.
- (11) Ramasubramaniam, A. Large excitonic effects in monolayers of molybdenum and tungsten dichalcogenides. *Physical Review B* **2012**, *86*, 115409.
- (12) Kormányos, A.; Burkard, G.; Gmitra, M.; Fabian, J.; Zólyomi, V.; Drummond, N. D.; Falko, V. $k \cdot p$ theory for two-dimensional transition metal dichalcogenide semiconductors. *2D Materials* **2015**, *2*, 022001.
- (13) Ciarrocchi, A.; Unuchek, D.; Avsar, A.; Watanabe, K.; Taniguchi, T.; Kis, A. Control of interlayer excitons in two-dimensional van der Waals heterostructures. *arXiv preprint arXiv:1803.06405* **2018**,
- (14) Hanbicki, A. T.; Chuang, H.-J.; Rosenberger, M. R.; Hellberg, C. S.; Sivaram, S. V.; McCreary, K. M.; Mazin, I.; Jonker, B. T. Double Indirect Interlayer Exciton in a $\text{MoSe}_2/\text{WSe}_2$ van der Waals Heterostructure. *arXiv preprint arXiv:1802.05310* **2018**,

- (15) Aivazian, G.; Gong, Z.; Jones, A. M.; Chu, R.-L.; Yan, J.; Mandrus, D. G.; Zhang, C.; Cobden, D.; Yao, W.; Xu, X. Magnetic control of valley pseudospin in monolayer WSe₂. *Nature Physics* **2015**, *11*, 148–152.
- (16) Aivazian, G.; Gong, Z.; Jones, A. M.; Chu, R.-L.; Yan, J.; Mandrus, D. G.; Zhang, C.; Cobden, D.; Yao, W.; Xu, X. Magnetic control of valley pseudospin in monolayer WSe₂. *Nature Physics* **2015**, *11*, 148.
- (17) Neumann, A.; Lindlau, J.; Colombier, L.; Nutz, M.; Najmaei, S.; Lou, J.; Mohite, A. D.; Yamaguchi, H.; Högele, A. Opto-valleytronic imaging of atomically thin semiconductors. *Nature Nanotechnology* **2017**, *12*, 329–334.
- (18) Glazov, M. M.; Amand, T.; Marie, X.; Lagarde, D.; Bouet, L.; Urbaszek, B. Exciton fine structure and spin decoherence in monolayers of transition metal dichalcogenides. *Physical Review B* **2014**, *89*, 201302.
- (19) Rivera, P.; Seyler, K. L.; Yu, H.; Schaibley, J. R.; Yan, J.; Mandrus, D. G.; Yao, W.; Xu, X. Valley-polarized exciton dynamics in a 2D semiconductor heterostructure. *Science* **2016**, *351*, 688–691.
- (20) Meier, F., Zakharchenya, B. P., Eds. *Optical Orientation*; North–Holland Physics Publishing, 1986.
- (21) Blackwood, E.; Snelling, M. J.; Harley, R. T.; Andrews, S. R.; Foxon, C. T. B. Exchange interaction of excitons in GaAs heterostructures. *Physical Review B* **1994**, *50*, 14246–14254.
- (22) Worsley, R. E.; Traynor, N. J.; Grevatt, T.; Harley, R. T. Transient Linear Birefringence in GaAs Quantum Wells: Magnetic Field Dependence of Coherent Exciton Spin Dynamics. *Physical Review Letters* **1996**, *76*, 3224–3227.